Accepted Manuscript

A novel hot embossing Graphene transfer process for flexible electronics

A. Ballesio, M. Parmeggiani, A. Verna, F. Frascella, M. Cocuzza, C.F. Pirri, S.L. Marasso

PII: S0167-9317(19)30036-X
DOI: https://doi.org/10.1016/j.mee.2019.02.010
Reference: MEE 10916

To appear in: *Microelectronic Engineering*

Received date: 19 October 2018
Revised date: 28 January 2019
Accepted date: 25 February 2019

Please cite this article as: A. Ballesio, M. Parmeggiani, A. Verna, et al., A novel hot embossing Graphene transfer process for flexible electronics, Microelectronic Engineering, https://doi.org/10.1016/j.mee.2019.02.010

A novel hot embossing Graphene transfer process for flexible electronics

A. Ballesio [a], M. Parmeggiani [a,b], A. Verna [a], F. Frascella [a], M. Cocuzza [a,c], C. F. Pirri [a,b] , S. L. Marasso [a,c]

[a] *Chilab - Materials and Microsystems Laboratory, DISAT, Politecnico di Torino, Chivasso (Turin), Italy*
[b] *Center for Sustainable Future Technologies, Italian Institute of Technology, Turin, Italy*
[c] *CNR-IMEM, Parco Area delle Scienze 37a, IT 43124, Parma, Italy*
alberto.ballesio@polito.it

***Abstract* - In this work a new Single Layer Graphene (SLG) transfer technique exploiting a hot embossing process was carried out. Flexible electrolyte gated Graphene Field Effect Transistors (G-FET) were fabricated and tested electrically. A polymeric transparent foil suitable for optics and flexible electronics, Cyclic Olefin Copolymer (COC) was used as flexible substrate. Raman characterization confirmed that the new Hot Embossing Graphene Transfer (HEGT) is suitable for the deposition of SLG and the fabrication of G-FETs. A Comparison with SLG common transfer method was carried out and proven for G-FETs fabrication. The HEGT devices showed typical characteristics and maintained the same performances when the substrate was bent. This demonstrated that the HEGT allows for efficient transfer of high quality SLG on large area thus providing the opportunity for the exploitation on a large scale production process for flexible substrates.**

Keywords - Graphene, CVD, Graphene transfer, flexible electronics, Hot Embossing, G-FET

1. Introduction

Graphene is one of the most studied 2D material and the application fields are widespread. Graphene based Field Effect Transistors (G-FET) are encountering a growing interest since they showed high performances as in liquid biosensors by functionalizing single layer (SLG) or few layer graphene (FLG) to detect biomolecules as DNA or proteins at very low concentration [1]–[3]. In recent years graphene has also been widely used in flexible electronics due to its high flexibility for the production of a wide variety of devices (solar cells, light-emitting diodes and field effect transistors) [4], [5], exploiting also wafer-scale processing strategies for back-gated G-FETs [6]. An integration on flexible substrates of G-FET for in liquid biosensing is more recent [7], on the contrary EGOFET (Electrolyte Gated Field Effect Transistors) or OECT (Organic Electro-Chemical Transistors), which are polymer based devices, have been commonly used on Kapton™ foils [8], [9] or on Polydimethylsiloxane (PDMS) [10] [11] or on textile fibers [12],[13]. The number of layers and defects in the SLG strongly influences the characteristics of the devices. The best known method to produce graphene with few layers and defects is Chemical Vapor Deposition (CVD) on Cu or Ni foils [14]; then a transfer strategy is needed to be properly deposited on the substrate containing the electrodes. The latter step is commonly performed using Poly(methyl methacrylate) (PMMA): after spinning it on the Cu foil, Cu is etched and graphene is deposited on the substrate; as a last step PMMA is etched and completely removed. This transfer process is a high critical operation [15] and one of the main issues for the exploitation of graphene at industrial level: the procedure is long and complex and cannot be automatized; moreover, at every step the graphene layer can degrade and PMMA contamination is very common, which worsen the sensors performances due to a n-type doping [16]. Therefore, alternative methods for the transferring process are required especially if flexible substrates are needed and handling and processing gets more complex. Graphene transfer by hot embossing has never been attempted, although hot embossing is a versatile and well known process for microsystem fabrication [17], [18]. In this work, a new method for graphene transfer exploiting hot embossing system was developed. The Hot Embossing Graphene Transfer (HEGT) consist in a molding of the copper where graphene has been growth on a Cyclic Olefin Copolymer (COC) foil containing the electrodes. After the complete removal of the copper the Graphene layer remains on the electrodes. By avoiding the PMMA sacrificial layer the processing steps are reduced. This paper focuses on this new approach compared to the more common fabrication one and explores the G-FET performances for flexible electronics.

2. Experimental

2.1. Graphene growth and G-FET fabrication

After rinsing 2 cm x 2 cm Cu foils in HCl to remove the native oxide, SLG was grown on them with a Moorfield NanoCVD 8G.

These SLG were transferred with two different techniques and the obtained devices were used to evaluate the differences between them.

A COC foil 140 µm thick (TOPAS 8007 X04) and a 4" SiO_2/Si wafer were used as substrates. 100 nm of Au were evaporated on both of them, with 10 nm of Ti as adhesion layer (Fig. 1, step a1 and b1). Electrodes were patterned by wet etching after UV photolithography with AZ 1518 positive photoresist (Fig. 1, step a2 a3 and b2 b3) with a channel 20 µm wide and 2 mm long.

The first transfer procedure employed the hot embossing technique (Fig. 1, step a4). The Cu foil with the SLG was embossed (model HEX01 JENOPTIK Mikrotechnik) on the COC foil with the already patterned electrodes at 80 °C with 10000 N of applied force for 120 s. Cu was removed by wet etching in a $FeCl_3$ solution for 20 min and samples were thoroughly rinsed twice in deionized (DI) water and once in HCl to remove any $FeCl_3$ residue, thus leaving the SLG on the Au electrodes (Fig. 1, step a5).

In the second transfer procedure, traditional PMMA-assisted transfer process was used to check the quality of the HEGT. A layer of PMMA (1.35% in anisole) was spin coated on the Cu foil side with the SLG. The Cu was then etched in a $FeCl_3$ solution. The Graphene/PMMA foil was cautiously rinsed as in the previous procedure and placed on the substrate (either COC or SiO_2/Si) (Fig. 1, step b4). Samples were dried under vacuum at room temperature to allow a better PMMA removal [19]. PMMA was then etched in acetone, leaving only the electrodes covered by the SLG (Fig. 1, step b5).

In both cases, by photolithography with AZ 1518 as positive photoresist, graphene was patterned by oxygen plasma for 30 s to remain only in the channel between source and drain.

For the passivation, polyamide (Asahi Kasei AM 271) was employed to avoid short circuits due to the electrolyte gating (Fig. 1, step a6 and b6). The final COC devices are reported in Fig. 2.

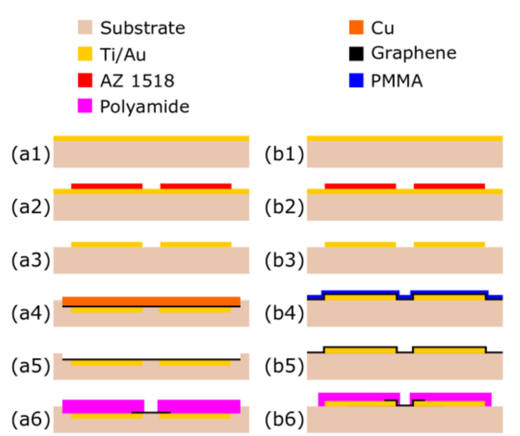

Figure 1: G-FET fabrication process flow via hot embossing (a1-a6) and common PMMA assisted transfer (b1-b6).

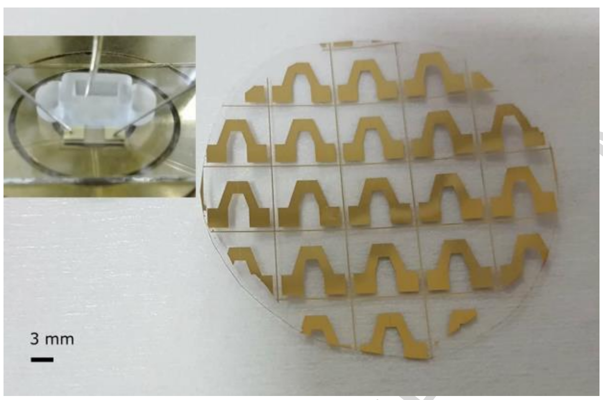

Figure 2: G-FET devices fabricated via hot embossing process of SLG on COC. In the inset: electrical characterization layout with PDMS well, source, drain and gate (Ag/AgCl leak free reference electrode) contacts.

2.2. Raman, Electrical and Atomic Force Characterization

In order to have a first evaluation of the quality of the graphene after the transfer processes, a Raman spectroscopy was performed on the final devices for graphene transferred via hot embossing on COC and via PMMA support on COC and on SiO_2/Si wafer.

Raman characterization has been performed with a Renishaw inVia Raman microscope (Renishaw plc, Wotton-under-Edge, UK) equipped with a Leica DMLM microscope with a 50x objective. The excitation was obtained with a 514.5 nm Ar laser with an output power of 50 mW (5 mW at the sample). All spectra were recorded using 5 accumulations (2 s exposure). To avoid photodegradation, the laser power density at the sample was decreased by increasing the diameter of the laser spot. To get the spectrum of SLG, a spectroscopy has been performed also onto the COC alone. Both the spectra were normalized with respect to the laser and then subtracted to get the specific graphene contribution.

The electrical characterization has been performed on three sets of devices, in order to analyze the influence of the transfer process and of the substrate. The characterized G-FETs were fabricated via PMMA assisted transfer on Si/SiO_2 substrate and on COC foil and fabricated via hot embossing on COC foil.

Electrical characterizations have been performed with a Keysight B2912A Source/Measure unit. The devices were tested with a probe station; to hold the electrolyte a PDMS well with a capacity of 50 µl was used, simply placed on the transistors. As a gate an Ag/AgCl leak free reference electrode was adopted, placing it in the well with the electrolyte.

The gate voltage was swept from -1 V to +1 V keeping the drain voltage fixed at different levels (20 mV, 70 mV, 120 mV, 170 mV, 220 mV) to measure in DI water the device trans-characteristics (drain current vs gate voltage). To make sure there was no leakage through the gate, the leakage current was measured in parallel and it was always more than 4 order of magnitude lower than the drain current.

Tests were then performed to study the response of the G-FETs made via hot embossing as flexible devices: the electrodes were folded upwards keeping the channel down with a curvature radius of 8 mm, and measurements were taken as previously described.

The AFM characterization was performed in tapping mode with Bruker Atomic Force Microscope, with probes with nominal resonance frequency of 300 KHz and elastic constant of 40 N/m.

3. Results and discussion

The novel HEGT was implemented and tested to obtain the final G-FETs on COC foil. The first fundamental result is the preserving of the SLG under the molding pressure necessary to the transfer (25 MPa). To obtain this, the HEGT should avoid any residual mechanical stress on the substrates. The low temperature and time selected in the process conditions induce a negligible polymer chains re-arrangement and hence no defects are transferred on the electrodes and SLG. The Raman spectrum of the graphene embossed on the COC (Fig. 3a) shows 3 main peaks: the D peak at 1343 cm^{-1}, the G one at 1572 cm^{-1} and the 2D at 2678 cm^{-1} and the I_{2D}/I_G ratio is 1,94. The ratio and the shapes of the 2D and G peaks demonstrate that the graphene is monolayer, while the presence of a small D peak means that few defects are present in the planar structure [20], [21]. As a comparison, the Raman spectrum of graphene PMMA transferred on COC (Fig. 3b) has the same peaks (D at 1346 cm^{-1}, G at 1576 cm^{-1} and 2D at 2687 cm^{-1}) as well as the one transferred on SiO_2/Si (Fig. 3c) (D at 1340 cm^{-1}, G at 1576 cm^{-1} and 2D at 2671 cm^{-1}).

From a comparison between the three spectra it can be seen that the ratio between 2D and G peaks is comparable, while the D peak is higher in the COC PMMA-transferred, meaning that there are more defects [20], [21].

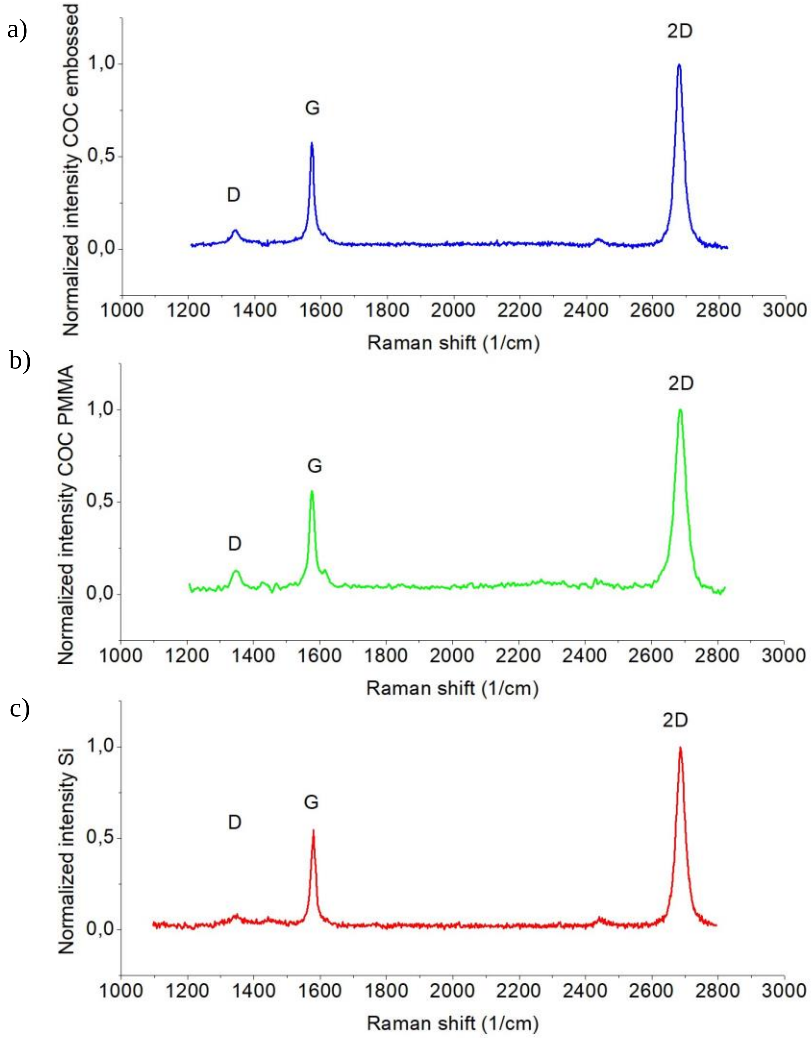

Figure 3: Comparison between normalized Raman spectra respectively of a) graphene transferred via hot embossing on COC, b) with PMMA on COC and c) with PMMA on SiO_2/Si.

In order to have more information on the graphene on COC, an AFM analysis was attempted (Fig. 4): valleys and hills in the range of tens of nm are due to the non-planar surface of the COC, which graphene covers. This is probably the reason of the D peak in the Raman spectrum and cause the slightly lower mobilities respect to SiO_2/Si samples.

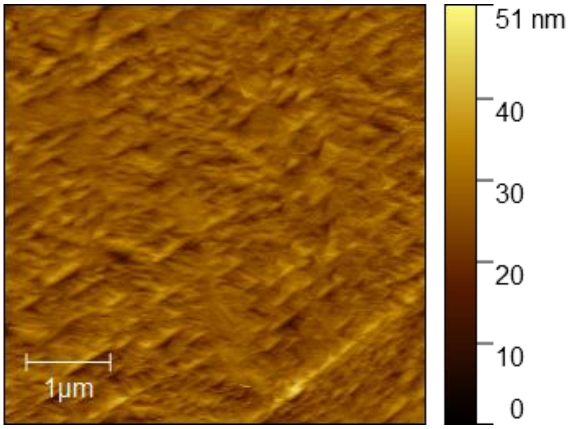

Figure 4: AFM analysis of graphene transferred on COC via hot embossing.

The tested G-FETs (Fig. 2) were fabricated following the HEGT and PMMA assisted procedures described in 2.1 with COC and Si/SiO_2 as substrates to evaluate the differences between the transfer processes. The PMMA-mediated transfer was used on both Si/SiO_2 and COC in order to analyze the influence of the polymer with respect to the common wafers.

The electrolyte-gated G-FETs fabricated via hot embossing show the typical ambipolar characteristics (Fig. 5a): the devices have the transition from p to n-type with the classical V-shape for the trans-characteristic. The shift of the Dirac points from the 0 V is probably due to a charging effect coming from the substrate as in the case of SiO_2 [22]. Improvements in the shift of the Dirac point could be achieved by using electrolytic delamination to avoid possible contaminations due to copper etching [23]. Mobilities were calculated by models already proposed by the literature for these kind of devices [24]–[26] with the transconductances obtained from the graphs. The results were μ_e = 141 cm^2/Vs and μ_h = 221 cm^2/Vs for embossed COC, μ_e = 87 cm^2/Vs and μ_h = 142 cm^2/Vs for transferred COC and μ_e = 178 cm^2/Vs and μ_h = 233 cm^2/Vs for transferred SiO_2/Si.

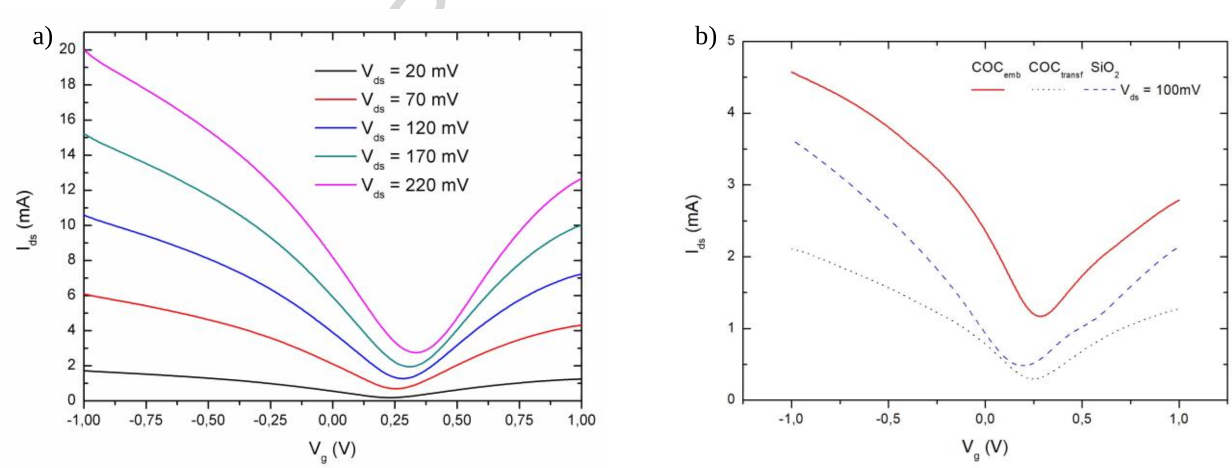

Figure 5: a) I_{ds} vs V_g of G-FET fabricated via hot embossing at different V_{ds} in DI water; b) Comparison of I_{ds} vs V_g characteristics in DI water at fixed drain voltage of G-FET fabricated via PMMA assisted transfer on Si/SiO_2 and COC and via hot embossing on COC.

The Dirac point of all three devices (PMMA-assisted transfer on COC and on Si/SiO_2 and via hot embossing on COC) are comparable, meaning that there are no significant charging effects (Fig. 5b). The COC PMMA-mediated transfer is the one showing the worst characteristics, having the lowest conductance and transconductance. This is probably due to the difficulty in the transfer arising from the flexibility of the substrate and increasing the possibility of fractures in the monolayer.

The embossed graphene shows a transconductance similar but slightly lower than the PMMA-assisted one on Si/SiO_2; that may be due to the physical stress that graphene has to endure during the embossing step, which may produce some fractures in the monolayer.

To test the performances as flexible devices for electronics, G-FETs fabricated via hot embossing were measured at first when flat and then were slightly folded and measured again. As it can be seen in Fig. 6, the device still has the common V-shape, meaning that it shows comparable performances when bent.

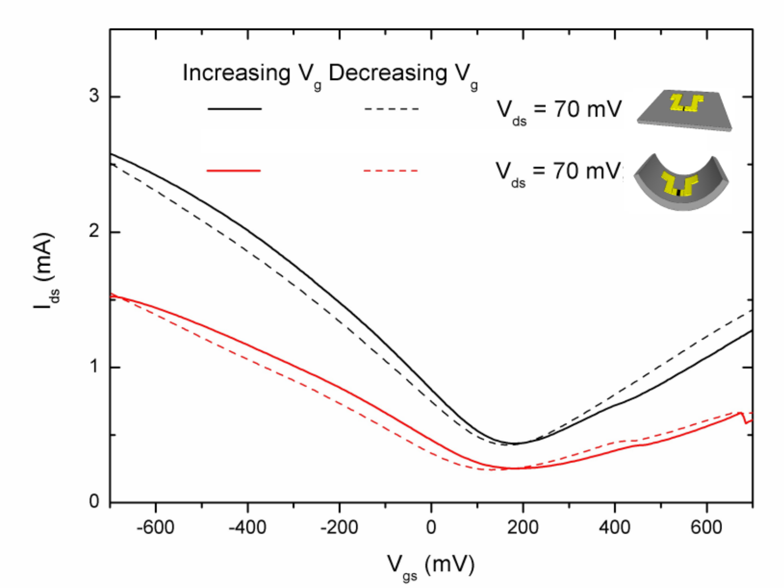

Figure 6: Comparison between the trans-characteristics of the same device with V_{ds} = 70 mV in standard configuration (black) and when folded (red).

4. Conclusion

In conclusion, a novel graphene transfer method via hot embossing at low temperatures (80 °C) has been successfully developed. A working G-FET on a COC flexible substrate was fabricated exploiting this method and showed valid performances also when folded with a curvature radius as low as 8 mm. Comparison between HEGT and common PMMA-mediated transfer technique shows comparable characteristics, thus demonstrating the possibility to efficiently transfer high quality SLG on flexible devices and to scale the production to an industrial level. Moreover, the G-FETs on flexible substrate are of great interest for the development of portable highly sensitive sensors for biomedical application.

5. AKNOWLEDGEMENTS

The present work was performed in the framework and financed by POLITO BIOMed LAB, an interdepartmental laboratory financed by Politecnico di Torino and DEFLeCT ("Advanced platform for the early detection of not small cells lung cancer", Piedmont "Health & WellBeing" Platform) project.

REFERENCES

[1] S. Xu *et al.*, "Real-time reliable determination of binding kinetics of DNA hybridization using a multi-channel graphene biosensor," *Nat. Commun.*, vol. 8, pp. 1–10, 2017.

[2] L. Zhou *et al.*, "Label-free graphene biosensor targeting cancer molecules based on non-covalent modification," *Biosens. Bioelectron.*, vol. 87, pp. 701–707, 2017.

[3] L. Zuccaro *et al.*, "Real-Time Label-Free Direct Electronic Monitoring of Topoisomerase Enzyme Binding Kinetics on Graphene," *ACS Nano*, vol. 9, no. 11, pp. 11166–11176, 2015.

[4] T.-H. Han, H. Kim, S.-J. Kwon, and T.-W. Lee, "Graphene-based flexible electronic devices," *Mater. Sci. Eng. R Reports*, vol. 118, pp. 1–43, Aug. 2017.

[5] N. Petrone, I. Meric, T. Chari, K. L. Shepard, and J. Hone, "Graphene field-effect transistors for radio-frequency flexible electronics," *IEEE J. Electron Devices Soc.*, vol. 3, no. 1, pp. 44–48, 2015.

[6] G. Fisichella *et al.*, "Advances in the fabrication of graphene transistors on flexible substrates," *Beilstein J. Nanotechnol.*, vol. 8, no. 1, pp. 467–474, Feb. 2017.

[7] Y. H. Kwak *et al.*, "Flexible glucose sensor using CVD-grown graphene-based field effect transistor," *Biosens. Bioelectron.*, 2012.

[8] D. Gentili *et al.*, "Integration of organic electrochemical transistors and immuno-affinity membranes for label-free detection of interleukin-6 in the physiological concentration range through antibody-antigen recognition," *J. Mater. Chem. B*, vol. 6, no. 33, pp. 5400–5406, 2018.

[9] P. D'Angelo *et al.*, "Nanomolar detection of the antitumor drug tamoxifen by flexible organic electrochemical devices," *AIP Conf. Proc.*, vol. 1990, 2018.

[10] X. Ji and P. K. L. Chan, "Highly sensitive glucose sensor based on organic electrochemical transistor with modified gate electrode," in *Methods in Molecular Biology*, 2017.

[11] S. W. Jeong, J. W. Jeong, S. Chang, S. Y. Kang, K. I. Cho, and B. K. Ju, "The vertically stacked organic sensor-transistor on a flexible substrate," *Appl. Phys. Lett.*, 2010.

[12] L. Rambausek, E. Bruneel, I. Van Driessche, and L. Van Langenhove, "Surface morphology of polyimide thin film dip-coated on polyester filament for dielectric layer in fibrous organic field effect transistor," *Autex Res. J.*, 2014.

[13] E. Battista *et al.*, "Enzymatic sensing with laccase-functionalized textile organic biosensors," *Org. Electron. physics, Mater. Appl.*, 2017.

[14] Y. Zhang, L. Zhang, and C. Zhou, "Review of Chemical Vapor Deposition of Graphene and Related Applications," *Acc. Chem. Res.*, vol. 46, no. 10, pp. 2329–2339, Oct. 2013.

[15] G. Borin Barin, Y. Song, I. de Fátima Gimenez, A. G. Souza Filho, L. S. Barreto, and J. Kong, "Optimized graphene transfer: Influence of polymethylmethacrylate (PMMA) layer concentration and baking time on graphene final performance," *Carbon N. Y.*, vol. 84, pp. 82–90, Apr. 2015.

[16] Y. Yu Wang and P. J. Burke, "A large-area and contamination-free graphene transistor for liquid-gated sensing applications," *Appl. Phys. Lett.*, vol. 103, no. 5, p. 052103, Jul. 2013.

[17] S. L. Marasso, G. Canavese, and M. Cocuzza, "Cost efficient master fabrication process on copper substrates," *Microelectron. Eng.*, vol. 88, no. 8, pp. 2322–2324, Aug. 2011.

[18] S. L. Marasso *et al.*, "A polymer lab-on-a-chip for genetic analysis using the arrayed primer extension on microarray chips.," *Biomed. Microdevices*, vol. 16, no. 5, pp. 661–70, Oct. 2014.

[19] M. Hinnemo *et al.*, "Scalable residue-free graphene for surface-enhanced Raman scattering," *Carbon N. Y.*, vol. 98, pp. 567–571, 2016.

[20] Y. ying Wang *et al.*, "Raman Studies of Monolayer Graphene: The Substrate Effect," *J. Phys. Chem. C*, vol. 112, no. 29, pp. 10637–10640, Jul. 2008.

[21] A. C. Ferrari, "Raman spectroscopy of graphene and graphite: Disorder, electron–phonon coupling, doping and nonadiabatic effects," *Solid State Commun.*, vol. 143, no. 1–2, pp. 47–57, Jul. 2007.

[22] P.-A. Haddad, D. Flandre, and J.-P. Raskin, "A Quasi-Static Model of Silicon Substrate Effects in Graphene Field Effect Transistors," *IEEE Electron Device Lett.*, vol. 38, no. 7, pp. 987–990, Jul. 2017.

[23] G. Fisichella, S. Di Franco, F. Roccaforte, S. Ravesi, and F. Giannazzo, "Microscopic mechanisms of graphene electrolytic delamination from metal

substrates," *Appl. Phys. Lett.*, vol. 104, no. 23, p. 233105, Jun. 2014.

[24] C.-C. Lu, Y.-C. Lin, C.-H. Yeh, J.-C. Huang, and P.-W. Chiu, "High Mobility Flexible Graphene Field-Effect Transistors with Self-Healing Gate Dielectrics," *ACS Nano*, vol. 6, no. 5, pp. 4469–4474, May 2012.

[25] S. Srinivasan, "ELECTRODE/ELECTROLYTE INTERFACES: STRUCTURE AND KINETICS OF CHARGE TRANSFER," in *Fuel Cells*, Boston, MA: Springer US, 2006, pp. 27–92.

[26] I. Meric, M. Y. Han, A. F. Young, B. Ozyilmaz, P. Kim, and K. L. Shepard, "Current saturation in zero-bandgap, top-gated graphene field-effect transistors," *Nat. Nanotechnol.*, vol. 3, no. 11, pp. 654–659, 2008.

- Graphene can be successfully transferred on COC without polymer sacrificial layer
- G-FETs show comparable characteristics to common transfer techniques
- G-FETs are suitable for flexible electronics since they work also under bending

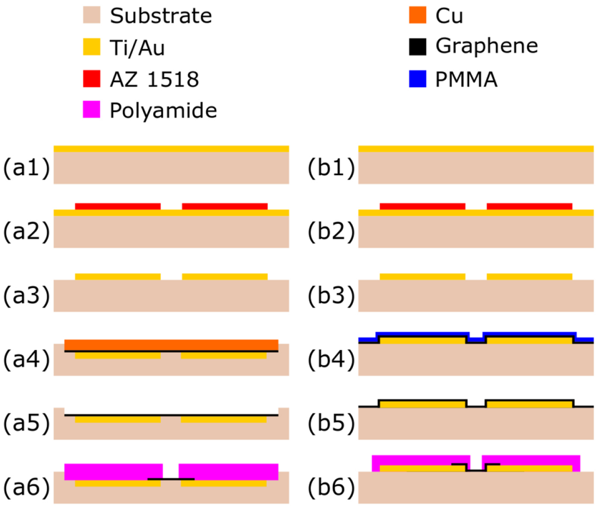

Substrate
Ti/Au
AZ 1518
Polyamide
Cu
Graphene
PMMA
(a1)
(a2)
(a3)
(a4)
(a5)
(a6)
(b1)
(b2)
(b3)
(b4)
(b5)
(b6)

Figure 1

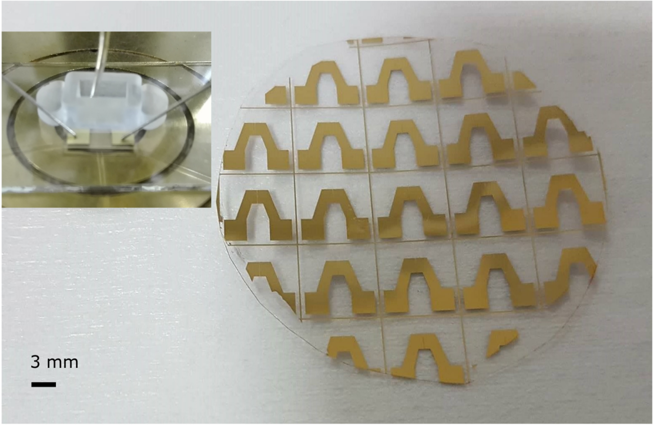

Figure 2

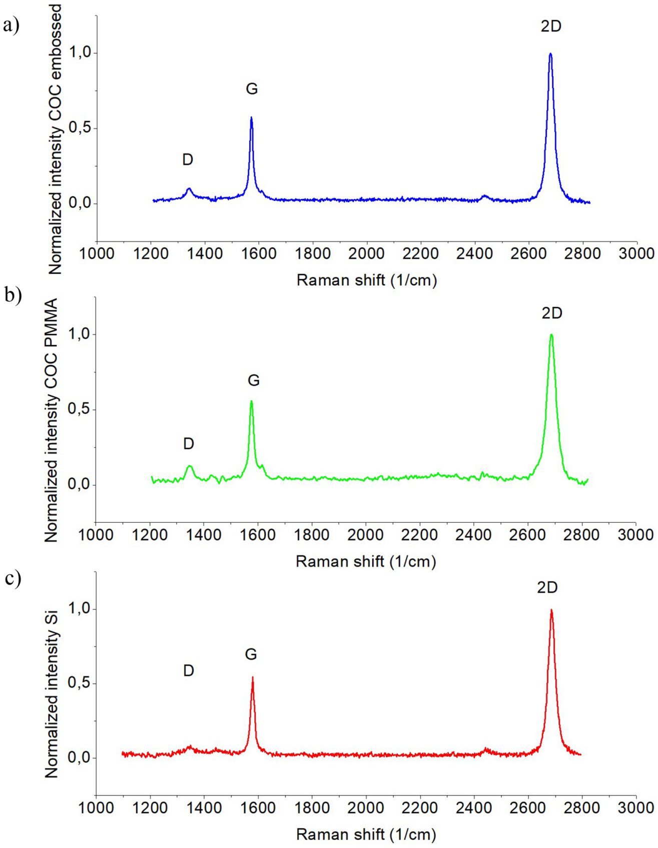

a)
Normalized intensity COC embossed
D
G
2D
1,0
0,5
0,0
1000
1200
1400
1600
1800
2000
2200
2400
2600
2800
3000
Raman shift (1/cm)
b)
Normalized intensity COC PMMA
D
G
2D
1,0
0,5
0,0
1000
1200
1400
1600
1800
2000
2200
2400
2600
2800
3000
Raman shift (1/cm)
c)
Normalized intensity Si
D
G
2D
1,0
0,5
0,0
1000
1200
1400
1600
1800
2000
2200
2400
2600
2800
3000
Raman shift (1/cm)

Figure 3

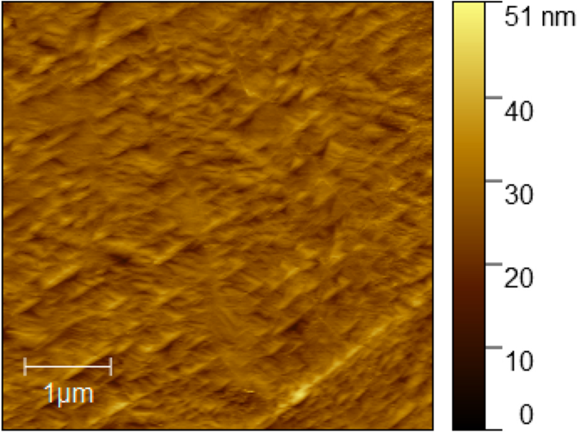

Figure 4

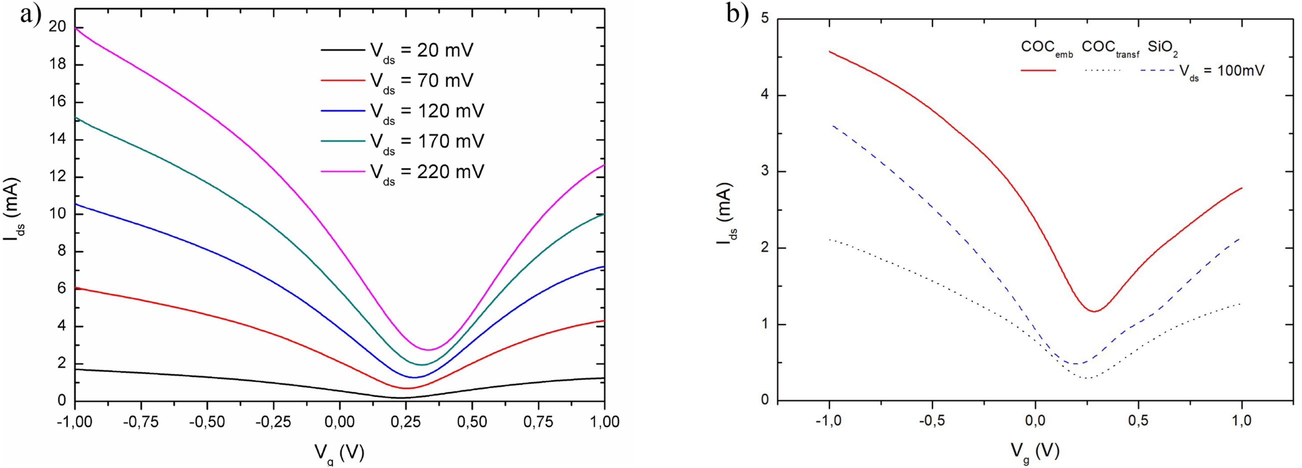

a)
V_{ds} = 20 mV
V_{ds} = 70 mV
V_{ds} = 120 mV
V_{ds} = 170 mV
V_{ds} = 220 mV
I_{ds} (mA)
V_g (V)
0
2
4
6
8
10
12
14
16
18
20
-1,00
-0,75
-0,50
-0,25
0,00
0,25
0,50
0,75
1,00
b)
COC_{emb} COC_{transf} SiO_2
V_{ds} = 100mV
I_{ds} (mA)
V_g (V)
0
1
2
3
4
5
-1,0
-0,5
0,0
0,5
1,0

Figure 5

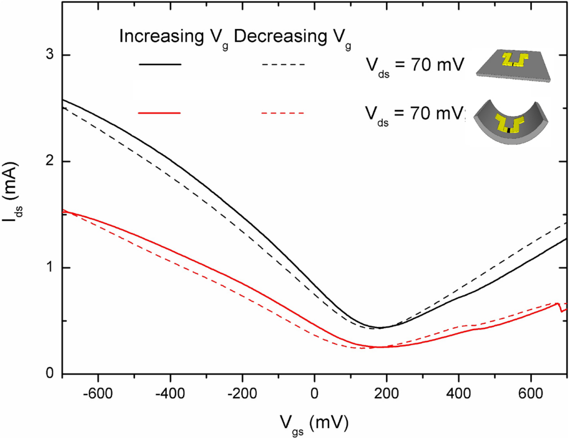
Increasing V g Decreasing V g
V ds = 70 mV
V ds = 70 mV
I ds (mA)
V gs (mV)
0
1
2
3
-600
-400
-200
0
200
400
600

Figure 6